RSC Advances

This is an *Accepted Manuscript*, which has been through the Royal Society of Chemistry peer review process and has been accepted for publication.

Accepted Manuscripts are published online shortly after acceptance, before technical editing, formatting and proof reading. Using this free service, authors can make their results available to the community, in citable form, before we publish the edited article. This *Accepted Manuscript* will be replaced by the edited, formatted and paginated article as soon as this is available.

You can find more information about *Accepted Manuscripts* in the Information for Authors.

Please note that technical editing may introduce minor changes to the text and/or graphics, which may alter content. The journal's standard Terms & Conditions and the Ethical guidelines still apply. In no event shall the Royal Society of Chemistry be held responsible for any errors or omissions in this *Accepted Manuscript* or any consequences arising from the use of any information it contains.

ROYAL SOCIETY OF CHEMISTRY

www.rsc.org/advances

The p-n heterojunction with porous $BiVO_4$ framework well-distributed Co_3O_4 for a super visible-light-driven photocatalyst

Xueming Dang, Xiufang Zhang*, Xiaoli Dong, Wenqi Ruan, Hongchao Ma, Mang Xue

School of Light Industry and Chemical Engineering, Dalian Polytechnic University, Dalian, China, 116034

* Corresponding authors. Tel.: +86 411 86323508; fax: +86 411 86323736. E-mail address: zhangxf@dlpu.edu.cn.

ABSTRACT: The p-n heterojunction with mesoporous $BiVO_4$ framework well-distributed Co_3O_4 is fabricated. The mesoporous structure is prepared by nanocasting technique using KIT-6 as template, while the incorporation of Co_3O_4 particles is completed by impregnation technique. Transmission electron microscopy (TEM) image shows that Co_3O_4 particles have been successfully loaded in the framework of the mesoporous $BiVO_4$. Energy dispersive spectrum (EDS) mapping displays that Co_3O_4 particles distribute uniformly in the sample, which is the result of the template effect of the mesoporous structure. The photocatalytic removal rate of RhB with $BiVO_4$ is enhanced by the construction of p-n heterojunction of Co_3O_4/mesoporous $BiVO_4$. This increase can be attributed to the enhanced separation efficiency of the photogenerated charge carriers produced by the p-n heterojunction. Mesoporous $BiVO_4$ make the guest material of Co_3O_4 to be well distributed, and the good dispersion of Co_3O_4 particles in the matrix of the mesoporous $BiVO_4$ provides large contact area of Co_3O_4 and $BiVO_4$, which promotes the charge transferring across the interface, thereby increases the

RSC Advances Accepted Manuscript

separation of electron-hole pairs, and leads to the enhancement of photocatalytic ability. Furthermore, mesoporous structure itself contributes to the enhanced photocatalytic performance.

1. Introduction

The semiconductor photocatalysis has attracted much attention due to its promising performance in environmental pollution control. [1-3] TiO_2 has been proved to be an excellent photocatalyst for the powerful photocatalytic activity and its outstanding stability. [4-6] However, the wide band gap (3.2 eV) of TiO_2 limits the utilization of visible light which accounts for a large part of the solar energy. $BiVO_4$, with a narrow band gap of 2.4 eV, has recently been focused on the photocatalytic field, which is satisfied with the basic requirements as a photocatalyst for pollution control, including being responsive to visible light [7] and very stable. [8, 9] However, low light absorption efficiency, and fast recombination of photogenerated electron-hole pairs still limit photocatalytic activity of $BiVO_4$. Therefore, some attempts have been devoted to improving the photocatalytic performance of $BiVO_4$, such as porous structure construction, [10, 11] noble metal modification,[12, 13] and heterojunction composite fabrication.[14, 15]

Coupling $BiVO_4$ with another semiconductor to form the heterojunction (especially p-n heterojunctions) can restrain the recombination of the photogenerated electron-hole pairs, and then, enhance the photocatalytic activity of $BiVO_4$. The large contact area of the two semiconductors can promote the charge transferring across the interface, thereby increase the separation of electron-hole pairs, and lead to the enhancement of photocatalytic ability. Thus, it is an ideal way to increase the contact area of semiconductors of the heterojunction for enhanced photocatalytic ability.[16]

Mesoporous structure construction can also enhance the photocatalytic performance.[17, 18] The construction of mesoporous structure in the bulk $BiVO_4$ can elevate the surface area of the photocatalyst to offer a large number of reactive sites.[19, 20] And also, it can enhance the light

RSC Advances Accepted Manuscript

absorption efficiency due to more photos distributed on the surface of the photocatalyst with the pores as the light transfer path. Besides, mesoporous materials itself can be used as a support of guest materials.[21] Mesopores in the structure can make the guest materials to be highly distributed, and restrain the generation of the guest materials to be small particles.[22, 23] High distribution and small particles of the guest materials in the framework of the host can all enhance the contact area of them. Inspired by this idea, Co_3O_4 is chosen as the guest material to be loaded in the mesoporous $BiVO_4$ to form the p-n heterojunction. It is a p-type semiconductor and a visible-light-driven photocatalyst with 2.07 eV of band gap.[24] The conduction band level (E_{CB}) of Co_3O_4 is +0.37 eV vs. NHE, which is more positive than that of $BiVO_4$ (E_{CB} = 0 eV vs. NHE) and the valence band (E_{VB}) level of Co_3O_4 is +2.44 eV vs. NHE, which is also more positive than that of $BiVO_4$ (E_{vB} = 2.40 eV vs. NHE). The matching of band levels and the types between Co_3O_4 and $BiVO_4$ makes Co_3O_4 to be a suitable material for constructing p-n heterojunction with $BiVO_4$.

Herein, Co_3O_4/mesoporous $BiVO_4$ p-n heterojunction with large contact area is firstly fabricated to get enhanced photocatalytic ability under visible light. The distribution role of mesoporous structure in Co_3O_4/mesoporous $BiVO_4$ as a visible-light-driven photocatalyst is discussed. RhB, a common pollutant in the industry wastewater, is chosen as a test substance to evaluate the photocatalytic performance of as prepared samples under visible light.

2. Experimental section

2.1. Sample preparation

2.1.1. Preparation of mesoporous silica KIT-6

The mesoporous silica KIT-6 with cubic Ia 3 d symmetry was prepared as follow: [25] 6 g of P123 was dissolved in 217 mL of distilled water, then 10 mL of concentrated HCl (35%) and

RSC Advances Accepted Manuscript

7.41 mL of butanol (99.4%) was added under stirring for 1 h at 35 ℃. 13.8 mL of TEOS (98%) was added at 35 ℃ (TEOS: P123: HCl: H_2O: BuOH = 1: 0.017: 1.83: 195: 1.31 in mole ratio). After stirred at 35 ℃ for 24 h, the mixture was transferred to an enclosed polypropylene bottle, for hydrothermal strategy at 100 ℃ for 6 h. The product was filtered and washed with deionized water and absolute ethanol for three times, and dried at 100 ℃ for 5 h. Finally, the solids were calcined at 550 ℃ (2 ℃/min) for 5 h.

2.1.2. Preparation of mesoporous $BiVO_4$

2 mmol of $Bi(NO_3)_3 \cdot 5H_2O$ was dissolved in 10 mL of 2 M HNO_3 under ultrasonic, and then, a transparent colorless solution was obtained. The same molar mass of NH_4VO_3 was added to the solution under ultrasonic for 30 min to form a bright yellow solution. Then 0.3 g of prepared KIT-6 was added. After complete immersion of the KIT-6, the mixture was put into the electrothermal constant-temperature dry box at 80 ℃ for 12 h to complete filling the $BiVO_4$ precursor into the void of KIT-6. The dried sample was then converted by calcination at 400 ℃ for 12 h. Finally, the mesoporous $BiVO_4$ was obtained with a 2 M NaOH aqueous solution to eliminate KIT-6. The final product was filtered and washed with distilled water and absolute ethanol. Reference $BiVO_4$ was prepared by the same procedure without the KIT-6.

2.1.3. Preparation of $Co_3O_4/BiVO_4$ composites

The loading Co_3O_4 on $BiVO_4$ was completed by the impregnation method from an aqueous solution of $Co(NO_3)_2$. The preparation of Co_3O_4/mesoporous $BiVO_4$ was carried out by the following typical procedure: mesoporous $BiVO_4$ powder (1.0 g) was added to 10 mL of solution of $Co(NO_3)_2$ containing an appropriate amount of $Co(NO_3)_2$ as 2% Co (recorded by S_1), 4% Co (recorded by S_2), and 6% Co (recorded by S_3) to $BiVO_4$ in a beaker. The suspension was stirred

RSC Advances Accepted Manuscript

during evaporation of water under the irradiation of an infrared light. The resulting powder was collected and calcined in air at 300 ℃ for 2 h. $Co_3O_4/BiVO_4$ was prepared by the same procedure with mesoporous $BiVO_4$ replaced by $BiVO_4$, and the mass percentage of Co to $BiVO_4$ was 4%.

2.2. Sample characterization

X-ray diffraction (XRD) spectra were recorded by Rigaku D/MAX-2400 with Cu Ka radiation, accelerating voltage of 40 kV, current of 30 mA. The scanning rate was 8° (2θ) min^{-1}, and the scanning range was 10-80°. Light absorption intensities were measured using a UV-vis spectrophotometer (Shimadzu, UV-2450) with a wavelength range of 200-800 nm. The micro-morphologies of the samples were got using a transmission electron microscopy (TEM; JEM-2100(UHR) JEOL). Energy dispersive spectrum (EDS) measurements were performed using a scanning electron microscope (SEM, JSM-6460LV) with an energy spectrometer (X-Max50). X-ray Photoelectron Spectroscopy (XPS) of the samples was obtained by X-ray photoelectron spectrometer (AMICUS). Fluorescence (FL) spectra were recorded by FL spectrometer (LS-55, PE). Tristar 3000 was used to examine the N_2 adsorption and desorption properties of as prepared samples at 77 K. The surface photovoltage spectra (SPS) were recorded by surface photovoltage measurement system, which consists of a monochromator (model Omni-λ3005) and a lock-in amplifier (model SR830-DSP) with an optical chopper (model SR540) running at a frequency of 20 Hz.

2.3. Measurement of photocatalytic activity

The photocatalytic activities of the as-obtained samples were monitored through the photodegradation of RhB under visible light irradiation. Photocatalytic reactions were conducted in a 100 mL cubic quartz reactor. A 300 W Xe lamp was employed as the visible light source. The light was passed through a filter, which should shield any wavelength below 420 nm. In all

RSC Advances Accepted Manuscript

experiments, photocatalysts (0.10 g) were added to 100 mL RhB aqueous solution (5 mg/L). During each photocatalytic experiment, 5 mL of the suspension was collected at predetermined time intervals. The suspension was centrifuged at 9500 rpm for 10 min, and the concentration of RhB in the supernatant was determined by measuring the absorbance at λ=553 nm with a Shimadzu UV2000 spectrophotometer. The adsorption ability of photocatalysts was measured under the same condition without the light illumination.

3. Results and discussion

3.1. Crystal structure

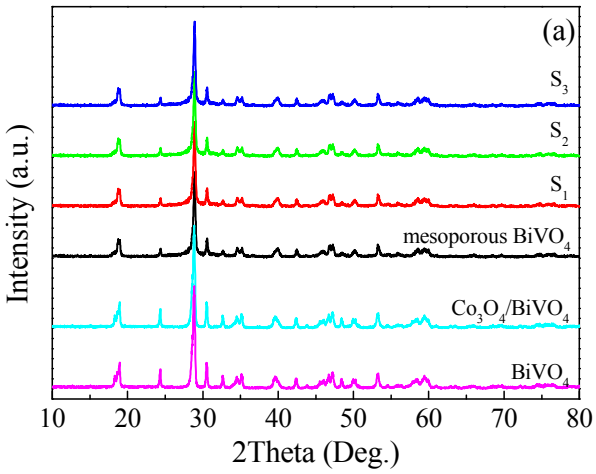

RSC Advances Accepted Manuscript

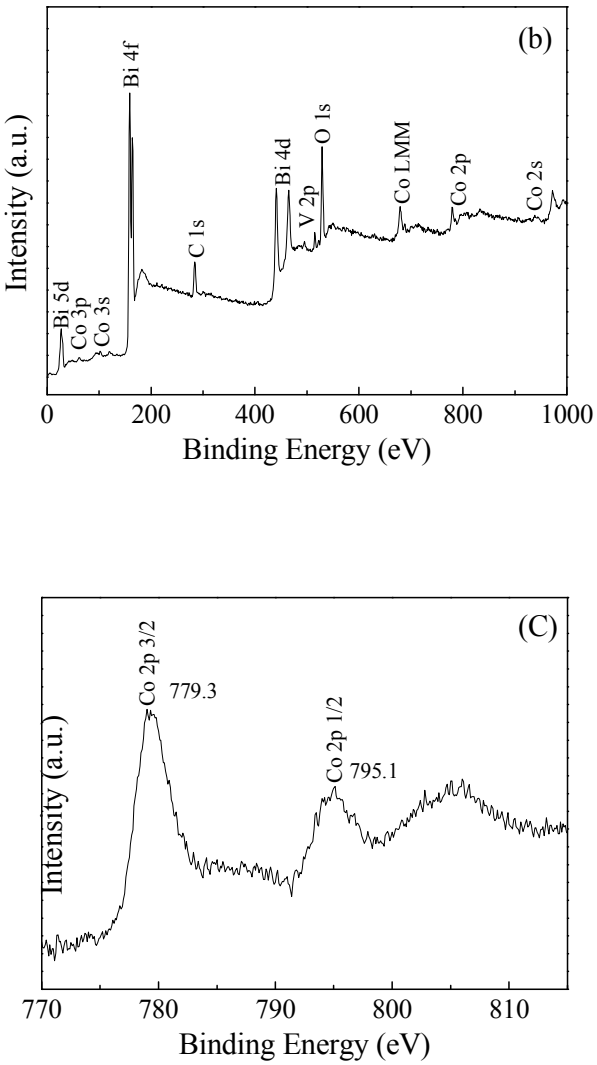

Fig. 1. (a) XRD patterns of $BiVO_4$, $Co_3O_4/BiVO_4$, mesoporous $BiVO_4$, S_1, S_2 and S_3 and XPS spectra of (b) S_2 and (c) Co_{2p} (high resolution).

The XRD patterns of $BiVO_4$, $Co_3O_4/BiVO_4$, mesoporous $BiVO_4$, S_1, S_2, and S_3 are shown in Fig. 1(a). Clear characteristic peaks with 2θ at 18.8°, 28.6°, 30.5°, 35.2°, 39.7° and 53.1° are observed. This indicates that $BiVO_4$ in the samples are monoclinic scheelite structure, which are indexed to the standard cards (JCPDS No.14-0688), and the processes of constructing mesoporous structure and loading Co_3O_4 cannot influence the crystal form of $BiVO_4$. No

RSC Advances Accepted Manuscript

diffraction peaks of Co species are observed over the composite samples, which is due to the small crystallite size or low concentration of Co species. To determine the existence and species of Co, XPS is recorded. XPS of S_2 is shown in Fig. 2 (b). The peaks ascribed to Bi, V, O and Co are found, certifying the existence of Co species. The high-resolution spectrum for Co_{2p} (Fig. 3(b)) shows two major peaks with binding energies at 779.3 and 195.2 eV, corresponding to Co $2p_{2/3}$ and $2p_{1/3}$, respectively, which is characteristic of a Co_3O_4. [26]

3.2. Morphologies

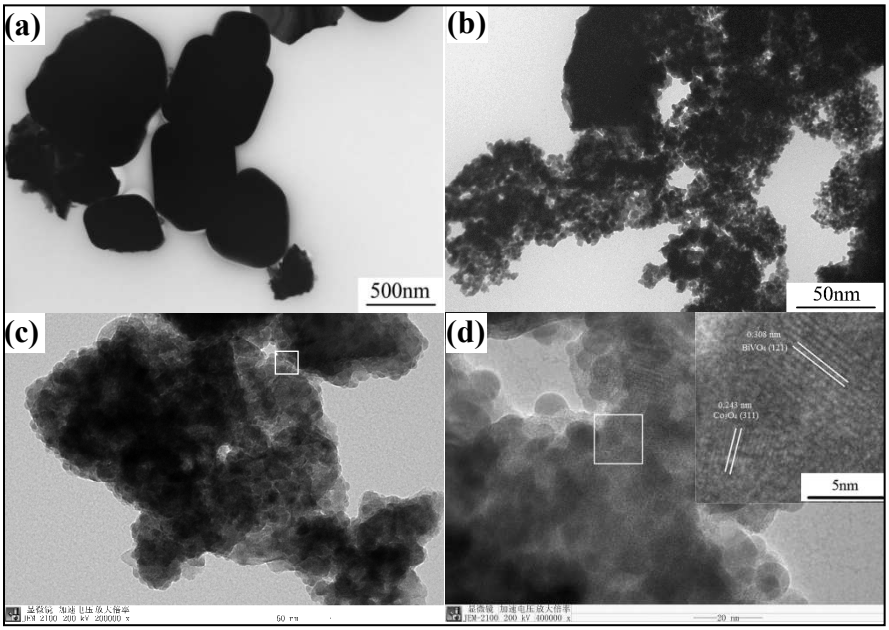

Fig. 2. TEM images of (a) $BiVO_4$, (b) mesoporous $BiVO_4$, (c) S_2 and (d) the rectangular area of (c), inset is the HRTEM image of the rectangular area of (d).

RSC Advances Accepted Manuscript

Fig. 3. EDS mapping of Co element of $Co_3O_4/BiVO_4$ (a) and S_2 (b).

The particle size of $BiVO_4$ based on TEM image (Fig. 2 (a)) is about 500 nm. The big particle and nonporous structure lead to low surface area of $BiVO_4$ (1.54 m^2). From Fig. 2(b), the replica of KIT-6 with many mesopores in $BiVO_4$ is found. The determined surface area of mesoporous $BiVO_4$ is 41.2 m^2/g, which is highly larger than that of $BiVO_4$. This enhancement can be attributed to the mesoporous structure and small size of the $BiVO_4$ particles. The big surface area of mesoporous $BiVO_4$ can apply more sites for the load of foreign materials. Fig. 2(c) and (d) shows typical TEM images of S_2. Most pores in mesoporous $BiVO_4$ are filled with Co_3O_4 particles. It can be measured from HRTEM image (inset of Fig. 2(d)) that d spacing are 0.308 and 0.243 nm, which are in agreement with the (121) plane of $BiVO_4$ and the (311) plane of Co_3O_4, respectively. It is apparent that Co_3O_4 particle has been successfully loaded in the mesoporous $BiVO_4$. To investigate the distribution of Co_3O_4 in mesoporous $BiVO_4$, the Co element distribution of $Co_3O_4/BiVO_4$ and Co_3O_4/mesoporous $BiVO_4$ is studied using EDS mapping. The EDS mapping image indicates that the Co element is well dispersed in Co_3O_4/mesoporous $BiVO_4$ (Fig. 3 (b)). This can be attributed to the template action of the mesoporous structure of the composite, which can highly distribute the guest materials and modulate the guest materials to be small particles. This good dispersion of Co element in the framework of mesoporous $BiVO_4$ can enhance the contact area of Co_3O_4 and $BiVO_4$, and thus,

RSC Advances Accepted Manuscript

elevate the photocatalytic ability of Co_3O_4/mesoporous $BiVO_4$. From Fig. 3(a), compared with that of Co_3O_4/mesoporous $BiVO_4$, some accumulation of Co element on $BiVO_4$ particles is found, suggesting the Co element in Co_3O_4/$BiVO_4$ is not well distributed. The proposed loading mechanism of Co_3O_4 on the surface of $BiVO_4$ and mesoporous $BiVO_4$ is illustrated in Scheme 1.

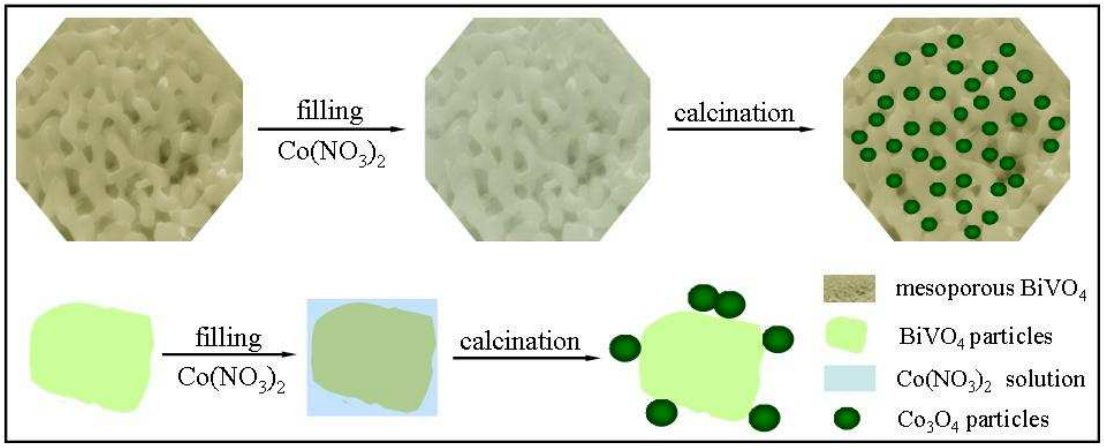

Scheme 1. The proposed loading mechanism of Co_3O_4 on the surface of $BiVO_4$ and mesoporous $BiVO_4$.

3.3. Separation ability of photogenerated charge carriers

RSC Advances Accepted Manuscript

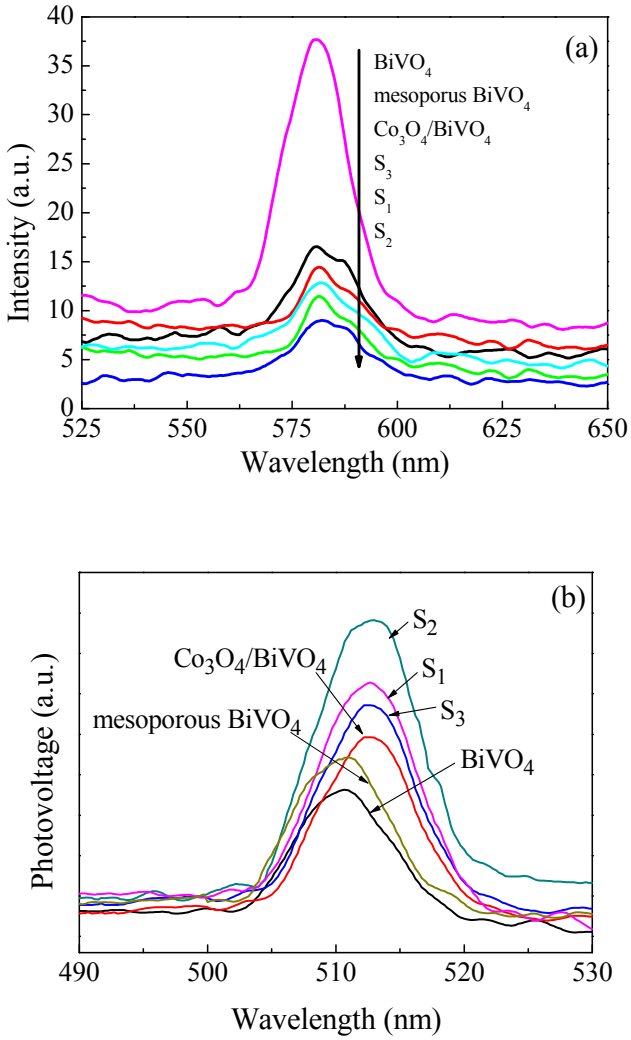

Fig. 4. (a) FL spectra and (b) SPS of $BiVO_4$, $Co_3O_4/BiVO_4$, mesoporous $BiVO_4$, S_1, S_2 and S_3.

FL analysis is used to reveal the separation efficiency of the photogenerated electrons [27] and holes in semiconductors, and the results are shown in Fig. 4(a). Considering that the FL emission results from the free charge carrier recombination, the lower peak indicates lower recombination rate of them. As can be seen from this figure, the FL intensity of $BiVO_4$ is the biggest one, inferring that $BiVO_4$ have the highest recombination rate of photogenerated charge carriers. The results confirm that the separation of photogenerated electrons and holes can be improved through the construction of mesoporous $BiVO_4$ or/and the formation of p-n heterojunctions

RSC Advances Accepted Manuscript

between Co_3O_4 and $BiVO_4$, leading to the enhancement of photocatalytic activity. The FL intensity of Co_3O_4/$BiVO_4$ is higher than those of Co_3O_4/mesoporous $BiVO_4$. Besides mesoporous structure, the big contact area of Co_3O_4/mesoporous $BiVO_4$ caused by the good distribution of Co_3O_4 in the composite contributes to the efficient separation of photogenerated of electrons and holes of Co_3O_4/mesoporous $BiVO_4$. The FL intensities of S_1, S_2 and S_3 are different, and S_2 gets the lowest. The reason why the FL intensity of S_1 is higher than S_2 is the lower content of Co, which affects the formation of enough p-n heterojunctions structure. However, introduction of too much Co_3O_4 into mesoporous $BiVO_4$, the pores and channels of samples may be crammed by Co_3O_4. Based on low recombination rate of S_2, it could be expected that S_2 should have high photocatalytic ability. SPS is one of indexes evaluating the separation efficiency of the photogenerated holes and electrons. [28] In general, the larger surface photovoltage the photocatalyst has, the more excellent separation ability of the photogenerated carriers the photocatalysts will be. The SPS are recorded, and the results are shown in Fig. 4(b). The result got by the analyses of FL is further confirmed by SPS result.

3.4. Optical absorption

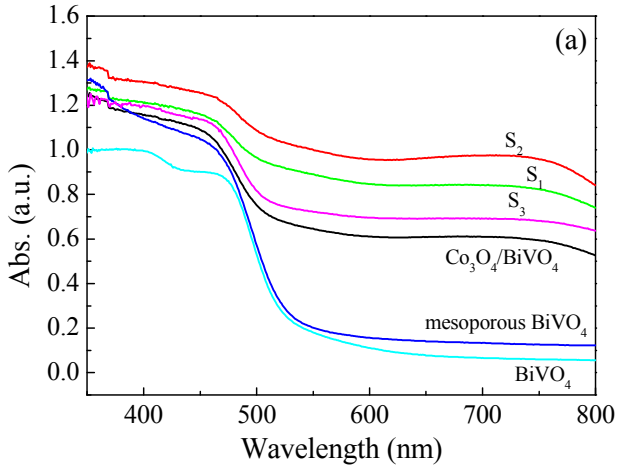

RSC Advances Accepted Manuscript

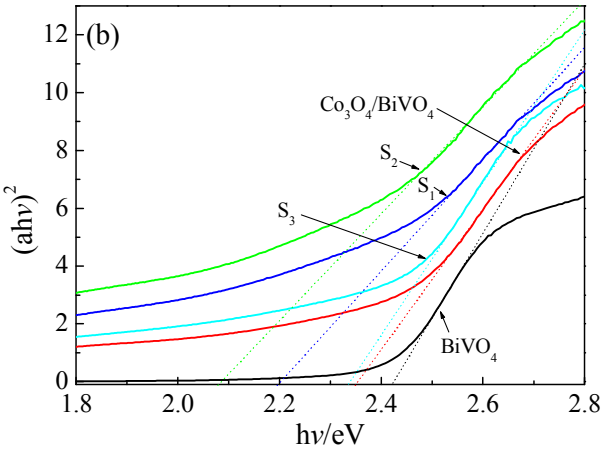

Fig. 5. (a) UV-vis absorption spectra of $BiVO_4$, $Co_3O_4/BiVO_4$, mesoporous $BiVO_4$, S_1, S_2 and S_3 and (b) calculation of the band gap by Kubelka-Munk function of $BiVO_4$, $Co_3O_4/BiVO_4$, S_1, S_2 and S_3.

The color of the Co_3O_4/mesoporous $BiVO_4$ composite powder is dark green and becomes darker and darker with enhanced Co content. The UV-vis diffuse reflectance spectra of the $BiVO_4$, $Co_3O_4/BiVO_4$, mesoporous $BiVO_4$, S_1, S_2 and S_3 are illustrated in Fig. 5(a). All the samples with mesoporous structure (mesoporous $BiVO_4$, S_1, S_2 and S_3) show enhanced absorption intensity over $BiVO_4$, indicating mesoporous structure is benefit to the absorption of the photos. This result has also been obtained in other published work.[29] And also, obvious red shifts of the band gap edge are found in the spectra of $Co_3O_4/BiVO_4$, S_1, S_2 and S_3. The calculated band gaps of $Co_3O_4/BiVO_4$, S_1, S_2 and S_3 are 2.34, 2.20, 2.09 and 2.31 eV (shown in Fig. 5(b)), which are smaller than that of $BiVO_4$ (2.43 eV). This should be attributed to the small band gap of Co_3O_4 (2.07 eV). Among Co_3O_4/mesoporous $BiVO_4$ composites, S_2 has the strongest absorption intensity and the narrowest band gap. Thus, under the same light intensity, S_2 can absorb more photos, and the enhanced photocatalytic ability can be anticipated.

3.5. Adsorption ability

RSC Advances Accepted Manuscript

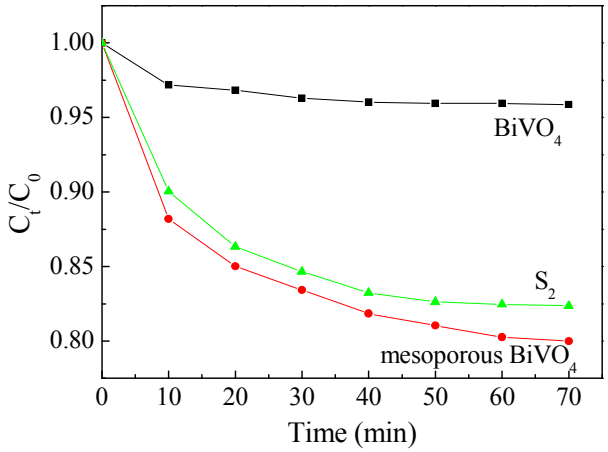

Fig. 6. RhB concentration C_t/C_0 vs. time for RhB adsorption.

Adsorption ability of the target substance is very important for the photocatalytic reaction. After 70 min, the removal rate of MB in the solution with mesoporous $BiVO_4$ is 20.0%, whereas that with $BiVO_4$ is 4.15%. It is obviously that the adsorption ability of $BiVO_4$ is enhanced by the construction of mesoporous structure, which can be attributed to the increase of the surface area. The adsorption ability of mesoporous $BiVO_4$ slightly decreases when Co_3O_4 is loaded on it. The decreased surface area of S_2 (29.3 m^2/g) results in this decline.

3.6. Photocatalytic activity and stability

RSC Advances Accepted Manuscript

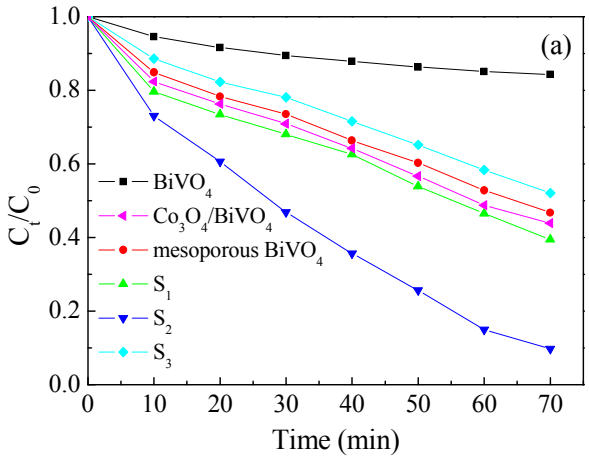

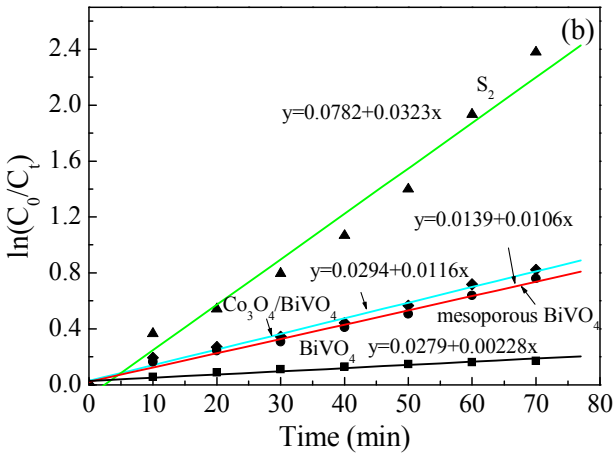

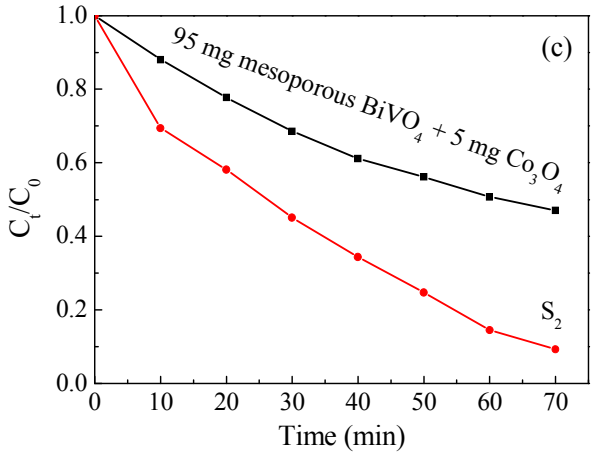

RSC Advances Accepted Manuscript

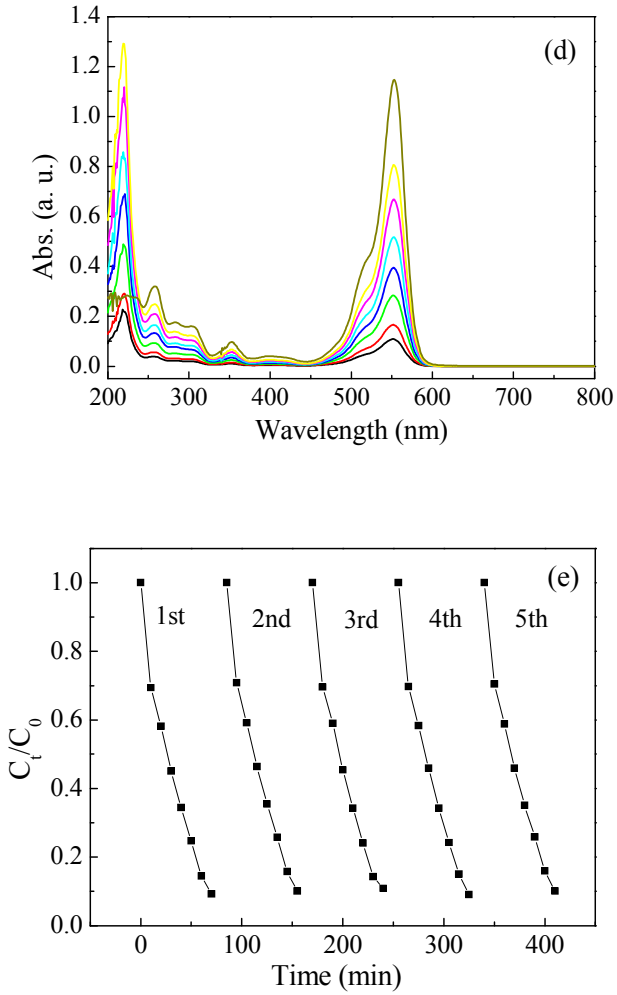

Fig. 7. RhB concentration C_t/C_0 (a) and $\ln(C_0/C_t)$ (b) vs. time for photocatalytic degradation of RhB with $BiVO_4$, $Co_3O_4/BiVO_4$, mesoporous $BiVO_4$, S_1, S_2 and S_3, RhB concentration C_t/C_0 vs. time for photocatalytic degradation of RhB with S_2 and the mixture of mesoporous $BiVO_4$ and Co_3O_4 (c), UV-vis absorbance spectra of RhB solution after photocatalytic degradation with S_2 (d) and cycling runs in the photocatalytic degradation of RhB with S_2 (e) under visible light irradiation.

In this experiment, RhB was adopted as a typical pollutant to evaluate the photocatalytic activity of photocatalysts under visible light irradiation. The variation of RhB concentration (C_t/C_0) vs. irradiation time with photocatalysts is shown in Fig. 7(a). In 70 min, only 15.7% of RhB is removed with $BiVO_4$, however, RhB removal rate with mesoporous $BiVO_4$ is 53.8%,

RSC Advances Accepted Manuscript

indicating that mesoporous structure can enhance the photocatalytic ability of $BiVO_4$. The kinetic analysis shows that the photocatalytic reaction with $BiVO_4$ can be considered as a first order reaction (see Fig. 7(b)), and calculated *k* value of mesoporous $BiVO_4$ is 0.0106 min^{-1}, which is higher than that of $BiVO_4$ (0.00228 min^{-1}). The enhanced light absorption ability, adsorption ability and separation efficiency of photogenerated charge carriers result in this increase. In 70 min, the RhB removal rate with S_2 is 90.3%. The *k* value of the S_2 (0.0323 min^{-1}) is nearly three times as big as that of mesoporous $BiVO_4$. The loading of Co_3O_4 on the mesoporous $BiVO_4$ to form the p-n heterojunction can enhance the photocatalytic performance of mesoporous $BiVO_4$. To confirm the heterojunction effect, the same amounts of mesoporous $BiVO_4$ (95 mg) and Co_3O_4 (5 mg) to those of S_2 are used as the photocatalyst to degrade RhB. Under the same condition, the RhB removal rate is largely lower than S_2 (Fig. 7 (c)), confirming that the enhanced photocatalytic ability of S_2 is attributed to the heterojunction effect. This enhancement can be attributed to the increased light absorption ability and separation efficiency of photogenerated holes and electrons. The loading quantity of Co_3O_4 affects the photocatalytic degradation ability of Co_3O_4/mesoporous $BiVO_4$. Among there Co_3O_4/mesoporous $BiVO_4$ composites, the removal rate of S_2 gets the highest one. But the determined RhB removal rate of S_3 is even lower than that of mesoporous $BiVO_4$, indicating that too much Co_3O_4 loaded on the surface of mesoporous $BiVO_4$ can decrease its photocatalytic ability. This result is beyond the explication based on the light absorption ability and the separation efficiency of photogenerated charge carriers. Thus, it is reasonably speculated that there are other factors that affect the photocatalytic ability of Co_3O_4/mesoporous $BiVO_4$. It is reported that the pores in the photocatalysts can accelerate the diffusion of the reactants, and then, promote the surface reaction of the photocatalysis.[30] The determined pore volumes of mesoporous $BiVO_4$ and S_3 are

RSC Advances Accepted Manuscript

0.0820 and 0.0615 cm^3/g, respectively, indicating loading Co_3O_4 can decrease the pore volume. And, some of pores of photocatalysts may be crammed. Thus, the surface reaction should be restrained, and the photocatalytic ability will decrease. To further analyze the role of mesoporous structure, the photocatalytic ability of $Co_3O_4/BiVO_4$ is compared with that of S_2. On one hand, the enhanced photocatalytic ability of S_2 can be attributed to the increase of light absorption ability, separation efficiency of photogenerated charge carriers and adsorption ability caused by the construction of the mesoporous structure. On the other hand, Co_3O_4/mesoporous $BiVO_4$ has large contact area of Co_3O_4 and $BiVO_4$, which can promote the charge transferring across the interface, thereby increase the separation of electron-hole pairs, and lead to the enhancement of photocatalytic ability.

It is well-reported that the RhB photodegradation occurs via two competitive processes: *N*-deethylation and the destruction of the conjugated structure. [31-33] The intermediates produced in RhB degradation process include DER, EER, DR and ER, which result from losing one and/or two ethyl groups from the xanthene ring in the parent RhB structure. If RhB is degraded by N-deethylation, these intermediates would be generated and the color of the oxidized RhB would change gradually from pink to green. On the other hand, if RhB is decomposed by destruction of the conjugated structure (cleavage of the chromophore structure), the maximum absorption wavelength of the solution during degradation will not obviously change. With the photocatalysis of S_2, the absorption maximum of the solution does not obviously shift (Fig. 7 (d)), indicating RhB is decomposed by destruction of the conjugated structure.

The stability of the Co_3O_4/mesoporous $BiVO_4$ composite (S_2) was also evaluated and the result is shown in Fig. 7 (e). After five recycles for the photocatalytic degradation of RhB, no

RSC Advances Accepted Manuscript

obvious loss of activity is found, indicating that Co_3O_4/mesoporous $BiVO_4$ composite is very stable and recyclable.

4. Conclusions

Co_3O_4/mesoporous $BiVO_4$ with mesoporous $BiVO_4$ networks containing well-dispersed Co_3O_4 particles is successfully fabricated. Construction of p-n heterojunction with mesoporous structure as the framework can enhance the photocatalytic ability of $BiVO_4$. Mesoporous $BiVO_4$ provides well-distributed space to host Co_3O_4 particles. High distribution of Co_3O_4 particles in the matrix of the mesoporous $BiVO_4$ provides large contact area of Co_3O_4 and $BiVO_4$, which promotes the charge transferring across the interface, thereby increases the separation of photogenerated electron-hole pairs, and leads to the enhancement of photocatalytic ability. Furthermore, mesoporous structure in $BiVO_4$ can enhance the photo absorption ability, adsorption ability and separation ability of photogenerated charge carriers, which contributes to the enhanced photocatalytic ability. Based on the results got here, it is confirmed that using mesoporous structure as the network to construct p-n heterojunction is an efficient way to enhance the photocatalytic ability.

Acknowledgments

This work was supported by the National Science Fund China (project no. 21107007) and Cultivation Program for Excellent Talents of Science and Technology Department of Liaoning Province (No. 2014026009).

References

[1] M. Sleiman, C. Ferronato and J.-M. Chovelon, *Environ. Sci. Technol*., 2008, 42, 3018-3024.

[2] L. F. Yin, J. F. Niu, Z. Y. Shen and J. Chen, *Environ. Sci. Technol*., 2010, 44, 5581-5586.

RSC Advances Accepted Manuscript

[3] Y. T. Lu, D. D. Wang, P. Yang, Y. K. Du and C. Lu, *Catal. Sci. Technol.,* 2014, 4, 2650-2657.

[4] H. Y. Zhu, Y. Lan, X. P. Gao, S. P. Ringer, Z. F. Zheng, D. Y. Song and J. C. Zhao, *J. Am. Chem. Soc*., 2005, 127, 6730-6736.

[5] X. B. Chen and S. S. Mao, *Chem*. *Rev*., 2007, 107, 2891-2959.

[6] J. H. Pan, Z. Lei, W. I. Lee, Z. Xiong, Q. Wang and X. Zhao, *Catal. Sci*. *Technol*., 2012, 2, 147-155.

[7] S. Tokunaga, H. Kato and A. Kudo, *Chem*. *Mater*., 2001, 13, 4624-4628.

[8] P. Madhusudan, M. V. Kumar, T. Ishigaki, K. Toda, K. Uematsu and M. Sato, *Environ*. *Sci*. *Pollut*. *R*., 2013, 20, 6638-6645.

[9] H. F. Lai, C. C. Chen,Y. K. Chang, C. S. Lu and R. J. Wu, *Sep*. *Purif. Technol.*, 2014, 122, 78-86.

[10] M. Ge, L. Liu, W. Chen and Z. Zhou, *Cryst. Eng. Comm*., 2012, 14, 1038-1044.

[11] H. Y. Jiang, H. D. Dai, X. Meng, K. M. Ji, L. Zhang and J. G. Deng, *Appl. Catal. B: Environ.,* 2011, 105, 326-334.

[12] S. Kohtani, J. Hiro, N. Yamamoto, A. Kudo, K. Tokumura and R. Nakagaki, *Catal*. *Commun*., 2005, 6, 185-189.

[13] A. P. Zhang and J. Z. Zhang, *J. Alloys. Compd.,* 2010, 491, 631-635.

[14] S. Ho-Kimura, S. J. A. Moniz, A. D. Handoko and J. W. Tang, *J. Mater. Chem. A*, 2014, 2, 3948-3953.

[15] H. Jiang, H. Endo, H. Natori, M. Nagai and K. Kobayashi, *Mater*. *Res*. *Bull*., 2009, 44, 700-706.

RSC Advances Accepted Manuscript

[16] H. T. Yu, S. Chen, X. F. Fan, X. Quan, H. M. Zhao, X. Y. Li and Y. B. Zhang, *Angew. Chem. Int. Ed.,* 2010, 49, 5106-5109.

[17] P. Manjula, R. Boppellam and S. V. Manorama, *ACS Appl. Mater. Interfaces,* 2012, 4, 6252-6260.

[18] Y. Ma, W. Tong, H. Zhou and S. L. Suib, *Micropor. Mesopor. Mat.,* 2000, 37, 243-252.

[19] Y. J. Chen, S. Lunsford and D. D. Dionysiou, *Thin Solid Films*, 2008, 516, 7930-7936.

[20] G. S. Li, D. Q. Zhang and J. C. Yu, *Chem. Mater.,* 2008, 20, 3983-3992.

[21] C. Y. Ma, Z. Mu, J. J. Li, Y. G. Jin, J. Cheng, G. Q. Lu, Z. P. Hao and S. Z. Qiao, *J. Am. Chem. Soc.*, 2010, 132, 2608-2613.

[22] X. D. Wang, D. R. G. Mitchell, K. Prince, A. J. Atanacio and R. A. Caruso, *Chem. Mater.*, 2008, 20, 3917-3926.

[23] Y. Wan, H. F. Yang and D. Y. Zhao, *Accounts. Chem. Res.,* 2006, 39, 423-432.

[24] M. C. Long, W. M. Cai, J. Cai, B. X. Zhou, X. Y. Chai and Y. H. Wu, *J. Phys*. *Chem*. *B*., 2006, 110, 20211-20216.

[25] L. Borchardt, E. Kockrick, P. Wollmann, S. Kaskel, M. M. Guron and L. G. Sneddon, *Chem*. *Mater*., 2010, 22, 4660-4668.

[26] Y. F. Sun, S. Gao, F. C. Lei,J. W. Liu, L. Liang, and Y. Xie, *Chem. Sci.,* 2014, 5, 3976-3982.

[27] S. F. Chen, W. Zhao, W. Liu, H. Y. Zhang, and X. L. Yu, *Chem. Eng. J.*, 2009, 155,466-473.

[28] Z. Y. Liu, D. D. Sun, P. Guo, and J. O. Leckie, *Nano Lett.,* 2007, 7, 1081-1085.

[29] X. F. Zhang, L. L. Du, H. Wang, X. L. Dong, X. X. Zhang, C. Ma and H. C. Ma, *Microporous*. *Mesoporous*. *Mater*., 2013, 173, 175-180.

RSC Advances Accepted Manuscript

[30] X. C. Wang, J. C. Yu, C. Ho, Y. D. Hou and X. Z. Fu, *Langmuir,* 2005, 21, 2552-2559.

[31] P. Lei, C. Chen, J. Yang, W. Ma, J. Zhao and L. Zhang, *Environ.Sci. Technol.,* 2005, 39, 8466-8474.

[32] C. C. Chen, W. Zhao, J. Li and J. Zhao, *Environ.Sci. Technol.,* 2002, 36, 3604-3611.

[33] H. B. Fu, S. C. Zhang, T. G. Xu, Y. F. Zhu and J. M. Chen, *Environ. Sci. Technol.,* 2008, 42, 2085-2091.

RSC Advances Accepted Manuscript

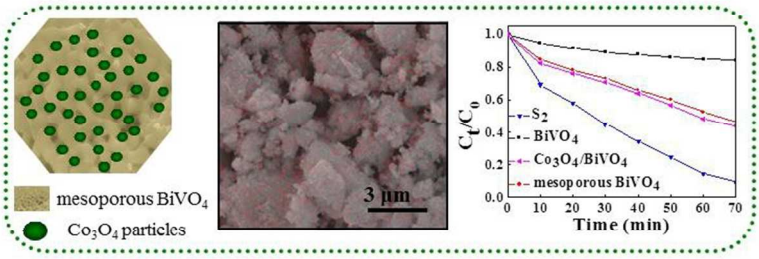

254x190mm (96 x 96 DPI)

RSC Advances Accepted Manuscript